Fish and Shellfish Immunology 90 (2019) 141–149

Contents lists available at ScienceDirect

Fish and Shellfish Immunology

journal homepage: www.elsevier.com/locate/fsi

Full length article

The microbiota profile and transcriptome analysis of immune response during metamorphosis stages in orange spotted grouper (*Epinephelus coioides*)

Joan Tang Xiao Joe[a,b], Pinwen Peter Chiou[c], Chia-Yu Kuo[a,b], Jacqueline Ho Jia Lin[c], Jen-Leih Wu[d], Ming-Wei Lu[c,e,*]

[a] Doctoral Degree Program in Marine Biotechnology, The College of Life Sciences, National Taiwan Ocean University, Keelung, Taiwan
[b] Doctoral Degree Program in Marine Biotechnology, Academia Sinica, Taipei, Taiwan
[c] Department of Aquaculture, National Taiwan Ocean University, Keelung, Taiwan
[d] Laboratory of Marine Molecular Biology and Biotechnology, Institute of Cellular and Organismic Biology, Academia Sinica, Nankang, Taipei, Taiwan
[e] Center of Excellence for the Oceans, National Taiwan Ocean University, Keelung, Taiwan

ARTICLE INFO

Keywords:
Epinephelus coioides
Metamorphosis
16s rRNA metagenomics
Intestinal microbiota
Immune system
Transcriptome analysis

ABSTRACT

Metamorphosis is a transformation process in larval development associated with changes in morphological and physiological features, including the immune system. The gastrointestinal tract harbors a plethora of bacteria, which might affect the digestion and absorption of nutrients, immunity, and gut-brain crosstalk in the host. In this study, we have performed metagenomic and transcriptomic analyses on the intestines of grouper at the pre-, mid- and post-metamorphosis stages. The sequencing data of 16S rRNA gene showed drastic changes in the microbial communities at different developmental stages. The transcriptomic data revealed that the leukocyte transendothelial migration and the phagosome pathways might play important roles in mediating immunity in grouper at the three developmental stages. This information will increase our understanding of the metamorphosis process in grouper larvae, and shed light on the development of antimicrobial strategy during larval development.

1. Introduction

The orange-spotted grouper, *Epinephelus coioides*, is a commercially important fish in many Asian countries [1]. In grouper larval development, metamorphosis is an essential and critical stage involved in the morphological and physiological changes [2]. During metamorphosis, the digestive system goes through significant changes, including the development of a functional stomach and increase in digestive capacity [3]. The metamorphosis process begins with the appearance of prolonged second dorsal section at 12 days post hatching (dph), and is complete by 50 dph. From 13 to 18 dph, the second dorsal section and pelvic fin spines become clearly visible and reach to their maximal lengths (Fig. 1). During the early developmental stage, the adaptive immunity is not yet fully established and functional. Hence, the innate immunity plays an important role in protecting the host against pathogens at the early developmental stage [4].

The intestinal mucosal immune system encounters more antigens than any other parts of the body do. The gastrointestinal tract is richly colonized by bacteria, archaea and eukaryotes, all together known as the gut microbiota [5]. The quantity of microorganisms living in the gut may reach over 95% of the total population in the whole body [6,7]. The gastrointestinal microbiota is known to produce beneficial components related to, for example, enhancing the immune system, protecting against pathogen, nutrition, and modulating host metabolism [8,9]. The gut microbiota produce short-chain fatty acids (SCFAs), such as propionate and butyrate, by fermentation of the non-digestible substrates like dietary fibers and endogenous intestinal mucus [10]. SCFAs can induce apoptosis of cancer cells, and regulate the intestinal gluconeogenesis; they also play an important role to maintain colon healthy [11]. Numerous evidences have demonstrated a network called “gut-brain axis”, in which bidirectional interactions between the gut microbiota and the central nervous system exist. Not only may the brain influence the function of the gut microbiota [12,13], but also alterations of microbiota composition may be associated with several disorders of the nervous system, including neuropsychiatric, neurodegenerative, and neuroinflammatory disorders [14]. As a result, gut

* Corresponding author. Department of Aquaculture, National Taiwan Ocean University, No.2, Beining Rd., Keelung, Taiwan.
E-mail address: mingwei@mail.ntou.edu.tw (M.-W. Lu).

https://doi.org/10.1016/j.fsi.2019.03.063
Received 4 January 2019; Received in revised form 26 March 2019; Accepted 26 March 2019
Available online 02 May 2019
1050-4648/

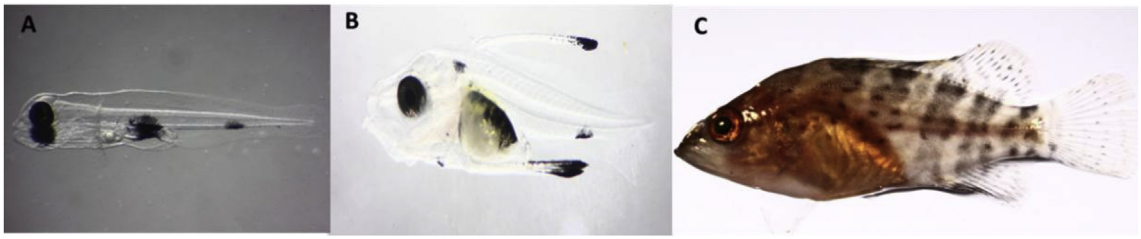

Fig. 1. The morphology of *E. coioides* during metamorphosis. (A) 12 days after hatching, the second dorsal started to lengthen. (B) 18dph, the second dorsal and pelvic fin spines were clearly visible and reach to the maximal length. (C) 50dph, transformation of larvae into juveniles occurred.

microbiota ultimately have a significant impact on the immunity, metabolism, diseases, brain and behaviors [15,16].

In recent years, metagenomics has become the major technique to study the intestinal microbiota in host [17]. To investigate the changes in intestinal microbiota and the development of immune system associated with metamorphosis in *E. coioides*, we have performed metagenomic and transcriptomic analyses on the intestines of fish at the pre-, mid and post-metamorphosis stages. The metagenomics data showed drastic changes in the microbial communities at different developmental stages. The transcriptomic data revealed pathways and molecules that might play important roles in mediating immunity in grouper at the three developmental stages. The new information will increase our understanding of the development of grouper larvae into juveniles, and further assist in the development of antimicrobial strategy in larvae going through the metamorphosis process.

2. Materials and methods

2.1. Experimental animals

In this study, fertilized eggs of orange-spotted grouper were collected from hatchery at Pingtung, Taiwan. The animal experiment was conducted at National Taiwan Ocean University (Keelung, Taiwan) by following the institutional IACUC guideline (Approve number: 106009). The tanks were stocked with *Chlorella* spp. prior to the installment of fertilized eggs. One gram of eggs was placed into a 100L tank with slightly aeration. The temperature was around room temperature with little photoperiod. Before 3dph, the first live feed provided to the larvae was ss-type live rotifers (*Brachionus plicatilis*), which were fed with *Chlorella* spp. From 3dph to 25dph, the larvae were fed with s-type rotifer; the L-type rotifers were fed to 25dph throughout 35dph juveniles. Subsequently, the juveniles were fed with *copepod nauplii* from 35dph to 50dph.

2.2. DNA extraction and 16S rRNA gene sequencing

The samples (12dph: n = 5group (150 fish pool together), 18dph: n = 4group (120 fish pool together), 50dph: n = 5group (4 fish pool together)) were collected and washed with sterile phosphate-buffered saline. The genomic DNA was extracted by using Genomic DNA Mini Kit, Geneaid. DNA concentration and purity were monitored on 1% agarose gel, and the concentration of DNA was diluted to 1ng/uL using sterile water. Distinct regions in 16S rRNA gene (16S V3—V4) were amplified using specific primers (16S V4: 515F-806R) with barcode. All PCR reactions were carried out with Phusion® High-Fidelity PCR Master Mix (New England Biolabs). PCR products were used to undergo quantification and qualification, mixed with equal volume of 1X loading buffer (contained SYBR green), and analyzed by electrophoresis on 2% agarose gel. Samples with bright main strip between 400 and 450bp were chosen for further experiments. The PCR products were mixed at equidensity ratios, and were purified with Qiagen Gel Extraction Kit (Qiagen, Germany). Sequencing libraries were generated using NEBNext Ultra DNA Library Pre ® Kit for Illumina by following manufacturer's recommendations, and the index codes were added. The library quality was assessed on the Qubit@ 2.0 Fluorometer (Thermo Scientific) and Agilent Bioanalyzer 2100 system (Agilent Technologies, Inc). At last, the library was sequenced on an Illumina platform and 250 bp paired-end reads were generated.

Data split paired-end reads was assigned to samples based on their unique barcode and truncated by cutting off the barcode and primer sequence. Sequence assembly paired-end reads were processed using FLASH (V1.2.7, http://ccb.jhu.edu/software/FLASH/) (Caporaso et al., 2010) to merge paired-end reads when at least some of the reads overlap the read generated from the opposite end of the same DNA fragment. The splicing sequences were afterwards called raw tags. Data Filtration Quality filtering on the raw tags were performed under specific filtering conditions to obtain the high-quality clean tags [18] according to the QIIME (V1.7.0, http://qiime.org/index.html) [19] quality-controlled process. Chimera removal the tags were compared with the reference database (Gold database, http://drive5.com/uchime/uchime_download.html) using UCHIME algorithm (UCHIME Algorithm, http://www.drive5.com/usearch/manual/uchime_algo.html) [20] to detect chimera sequences, and then the chimera sequences were removed [21] to obtain Effective Tags.

OTU Production Sequences analysis were performed by Uparse software (Uparse v7.0.1001, http://drive5.com/uparse/) [22]. Sequences with ≥97% similarity were assigned to the same OTUs. Representative sequence for each OTU was screened for further annotation. Species annotation for each representative sequence, the GreenGene Database (http://greengenes.lbl.gov/cgi-bin/nph-index.cgi) [23] was used based on RDP 3 classifier (Version 2.2, http://sourceforge.net/projects/rdp-classifier/) [24] algorithm to annotate taxonomic information. Data Normalization OTUs abundance information was normalized using a standard of sequence number corresponding to the sample with the least sequences. Subsequent analysis of alpha diversity and beta diversity were all performed based on this output normalized data. The KEGG pathway used an OTU table that had already been generated for use with PICRUSt. PICRUSt currently can only use an OTU table with GreenGene OTU identifiers which is the output from closed-reference picking or by filtering out de-novo OTUs after open-reference picking. Statistical significance was accepted at $p < 0.05$, and high significance was accepted at $p < 0.01$.

Alpha diversity is applied in analyzing complexity of species diversity for a sample through indices, including Observed-species, Chao1, Shannon, Simpson, ACE, and Good-coverage. All these indices in our samples were calculated with QIIME (Version 1.7.0) and displayed with R software (Version 2.15.3). Two indices were selected to identify the community richness. First is the Chao1 estimator (Chao) (http://www.mothur.org/wiki/Chao); second, Abundance-based Coverage Estimator (ACE) (http://www.mothur.org/wiki/Ace). The ACE incorporated data from all species with fewer than 10 individuals, rather than just singletons and doubletons (Anne Chao, 1992). Two indices were used to identify the community diversity. First, Shannon - the Shannon index (http://www.mothur.org/wiki/Shannon); second is Simpson - the Simpson index (http://www.mothur.org/wiki/Simpson). The Shannon index is an information statistic index, which means it

assumes all species are represented in a sample and that they are randomly sampled. The Simpson index is a dominance index for it gives more weight to common or dominant species. In this case, a few rare species with only a few representatives will not affect the diversity. Cluster analysis was preceded by principal component analysis (PCoA), which was applied to reduce the dimension of the original variables using the FactoMineR package and ggplot2 package in R software (Version 2.15.3).

2.3. RNA isolation, transcriptome assembly and pathway review

Total RNA from the grouper (12dph:n = 150, 18:n = 120, 50dph:n = 4) was extracted by using TRIzol (life technologies), according to the manufacturer's protocol. RNase-free DNase I (GMbiolab, Taiwan) was used to remove the residual genomic DNA. Then, RNA concentration and quality were verified by using Agilent 2100 Bioanalyzer. The extracted RNA was stored at −80 °C until processed for library preparation. After RNA extraction, RNA was quantified to 150ng/ul and total RNA was fixed to be 20 μg. Later, transcriptome sequencing was carried out by the company Genomics using Illumina Hiseq™ 2000. The data formed was proceeded using software CLC Genomics Worbench while reads were assembled and the expressions of genes were analyzed. Log_2 fold change and FDR p-value were obtained from the result.

Using FDR p-value ≤ 0.001 and Log_2 fold change abs value > 2, data was filtered and output as a csv file. R language (R v3.3.0) was used in order to form the data analysis graph while gene annotation was done using ncbi-blast + v2.3.0. Bioconductor v3.3 worked as a tool to find out the gene function and pathway related through Gene Ontology (GO) and KEGG database.

2.4. RNA isolation and gene expression

After RNA extraction, 1 μg of total RNA was used for cDNA synthesis by using HiScript I Reverse Transcriptase (BIONOVAS, Canada). Reverse transcription was conducted, according to the manufacturer's protocol with an Oligo $(dT)_{18}$ primer. The synthesis condition of cDNA was set at: 65 °C for 5 min, 42 °C for 60 min and 70 °C for 15 min. Quantitative real-time PCR (qPCR) was performed using the Applied BiosystemTM 7500 Real-Time PCR System (Applied Biosystems, USA) on a TOptical Thermocycler ® (Analytik Jena AG, Germany). The qPCR reaction contains 1 μl of the cDNA template, 10 μl of the 2X qPCRBIO syGreen Master Mix, 0.8 μl each of the forward and reverse primer (10pmol/uL) shown in Table .2. The amplification condition was initial denaturation at 95 °C for 5 min, followed by 40 cycles of 95 °C for 5sec, 65 °C for 30sec. The melting curve and cooling were performed at the last step of qPCR. The primers used in this study were listed in Table 1. The expression levels of the target gene were normalized to beta-actin, a housekeeping gene. Fold change in the relative gene expression with control group was determined by the standard $2^{-\triangle\triangle Ct}$ method. The changes were analyzed by unpaired sample *t*-test. Statistical significance was accepted at $p < 0.05$, and high significance was accepted at $p < 0.01$. All data were expressed as mean ± standard deviation (mean ± SD).

3. Results

3.1. The intestinal bacterial diversity and richness in grouper at different metamorphosis stages

The species accumulation boxplot was used to evaluate the adequacy of sample size and the species richness. As shown in Fig. 2, with the increase in sample size the boxplot showed first a sharp rise that later approached to a plateau at the sample size of 28, indicating adequate sample numbers in the metagenomic analysis. The alpha diversity indices (Chao1, ACE, Shannon and Simpson) were further analyzed to estimate the microbiome richness and diversity in the intestine flora of grouper at the three different metamorphosis stages (Table .1). The varieties in the intestinal bacterial communities at 50dph were significantly decreased as compared to that at 12dph and 18dph. The microbiomes diversity and richness at 18dph were higher than those at 12dph and 50dph.

Table 1
Sequences of primers used in the present study.

Primer Name	Orientation	Nucleotide Sequences (5′-3′)	Primer Usage
341F	sense	CCTAYGGGRBGCASCAG	amplify V3−V4 region
806R	antisense	GGACTACNNGGGTATCTAAT	amplify V3−V5 region
beta-actin	sense	TCCACCgCAAATgCTTCTAA	real-time PCR
beta-actin	antisense	TgCgCCTgAgTgTgTATgA	real-time PCR
NF-kB	sense	CAGGACGGCAACGGAGA	real-time PCR
NF-kB	antisense	TGCTGCTGACTGCTGAG	real-time PCR
TLR3	sense	CTggCTTACTACAACCACCCC	real-time PCR
TLR3	antisense	CAAACTCCCTgCCCTCTTCA	real-time PCR
IL-1B	sense	CCAGCGTTGAGGGCAGAA	real-time PCR
IL-1B	antisense	ATCGTCTCCAGATGTAAGGTT	real-time PCR
INF-1	sense	CTgTgTCCTTCCCgAATCAT	real-time PCR
INF-1	antisense	gTgCAgCTTCTTgCTCTCCT	real-time PCR
IFN-2	sense	TggAggCgTACgAAAAgCTg	real-time PCR
IFN-2	antisense	gCTCgTTgTACCggTgTTTC	real-time PCR
Mx gene	sense	ATTgTCAggTgCAgAggTCA	real-time PCR
Mx gene	antisense	TCTTTCAgCCAgCTCAggAA	real-time PCR

Table 2
The microbial diversity index including Shannon, Simpson, Chao1 and ACE of 16S rRNA sequence library. Shannon and Simpson index is used to identify bacterial community diversity; besides, Chao1 and ACE is used to identify bacterial richness.

samples	Shannon	Simpson	Chaol	ACE
12dph	5.285	0.884	1161.416	1178.623
18dph	7.457	0.972	1613.39	1622.872
50dph	1.599	0.363	697.802	785.861

3.2. Comparison of the intestinal bacterial communities among grouper at different metamorphosis stages

The principal component analysis (PCA) was conducted to observe the composition of intestinal flora communities. PCA is a statistical procedure to extract principle components and structures in data by using orthogonal transformation and reducing dimensionalities of data [25]. The more similar the compositions among the sample sets are, the closer the distance of their corresponding data points on the PCA graph are. Fig. 3 shows that the individuals collected at 12, 18 and 50dph were clustered in three distinct areas, indicating significant variation in the intestinal bacterial composition among the three groups. The 16s rRNA gene sequencing data (Fig. 4A) further revealed that at the phylum level *Proteobacteria* is the most abundant species in the midgut, with an abundancy of 86%, 70% and 96% in the fish at 12dph, 18dph and 50dph, respectively. *Firmicutes* was the second most abundant microbe at 12dph (4%) and 18dph (6%). *Actinobacteria*, *Bacteroidetes* and *Chloroflexi* were also abundant in the microbiota at 18dph. The rest of the microbiome at 50dph consisted of minor amount of *Firmicutes*, *Acidobacteria*, *Actinobacteria* and *Bacteroidetes*. We further analyzed the relative abundance of microbes in the intestine at the genus level. The top 35 dominant genera among all samples was displayed in a species abundance heat map (Fig. 4B). Red color indicates high abundance genera and blue color low abundance. At 12dph, the *Exiguabacterium* and *Acinetobacter* were two most dominant bacteria. There were 7 abundant genera at 18dph, that is, *Propionibacterium*, *Marivita*, *unidentified-Holosporacaea*, *Idiomarinas*, *Halomonas*, *Caldisericum*, and

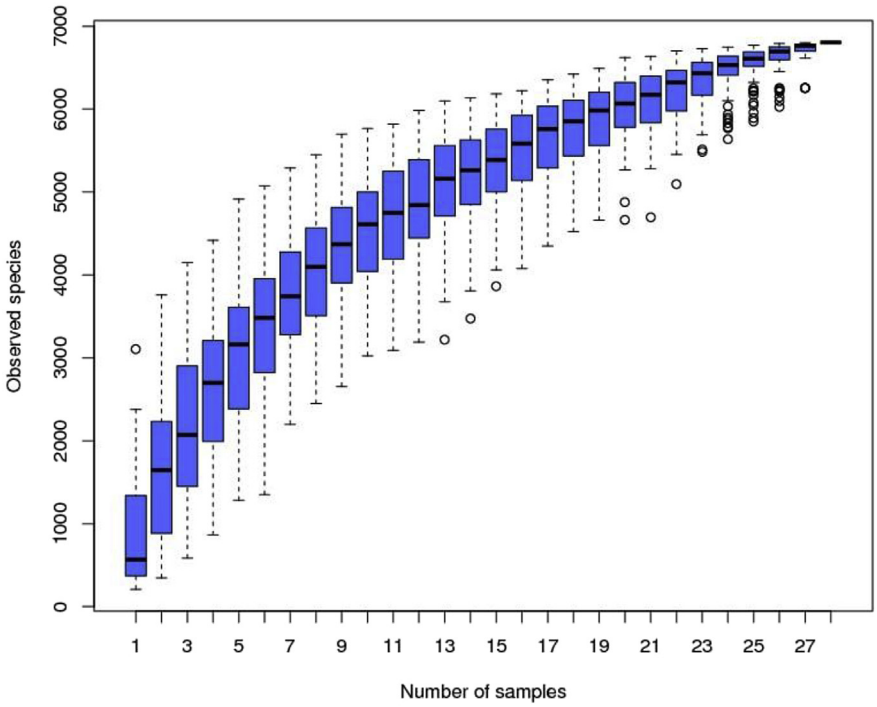

Fig. 2. The diversity and richness of the intestinal flora in *E. coioides*. (A) Species accumulation boxplot: The plot demonstrates the adequacy of sample size and the species richness. Plotted by the "Sample number" on the X-axis and "OTU number" on the Y-axis.

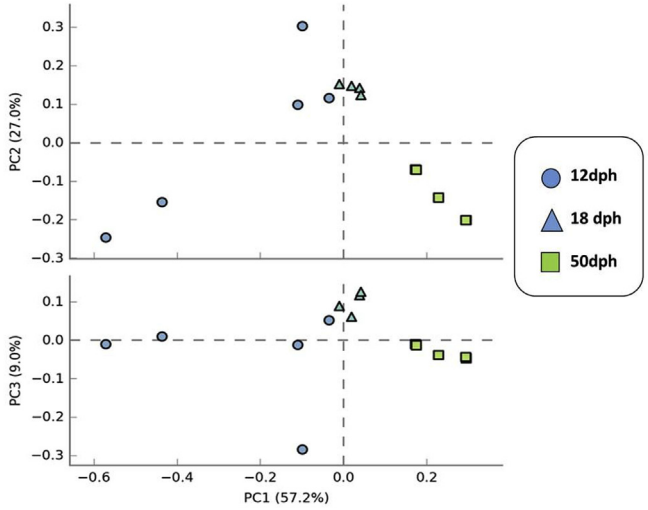

Fig. 3. Principal component analysis (PCA): each point represents a sample, plotted by the second principal component on the Y-axis and the first principal component on the X-axis, which was colored by group.

Nitrosomonas. At 50 dph, *Desulfovibrio* and *Photobacterium* were the two most dominant genera. The comparison of intestinal bacterial communities among grouper at different developmental stages was further conducted by the Venn diagram. As shown in Fig. 5, the OTU number at 12, 18 and 50dph was 682, 1285 and 388, respectively. The number of OTUs shared by all three groups was 701. In addition, the number of unique OTUs between 12dph and 18dph, 18dph and 50dph, 12dph and 50dph, was 929, 339 and 96, respectively.

3.3. Biological pathways affected in the intestines of grouper at different metamorphosis stages

The NGS data was further subjected to analysis against KEGG to reveal the biological pathways that were affected in the intestines of grouper at different metamorphosis stages. The results showed that pathways relevant to leukocyte, lysosome and phagosome were the most affected pathways between grouper at 12dph and 50dph (Fig. 6A). Further analysis of the transcriptomes showed that the leukocyte transendothelial migration pathway and the phagosome pathway were the two most significantly activated pathways. In the leukocyte transendothelial migration pathway, four genes (Rap1, β-catenin, JAM2 and Actin) were significantly up-regulated while two genes (p120ctn and CAMs) down-regulated (Fig. 6B). In the phagosome pathway, significant up-regulation of F-actin, ATPase, TUBA and NOS was observed (Fig. 6C).

3.4. The gene expression of immune system at the metamorphosis stages

Quantitative real-time RT-PCR was conducted to assay the expression of representative immune genes in whole larvae at 12 and 18dph, and in the spleen, brain and head kidney in juveniles at 50dph. The results showed the expression level of NF-κβ was slightly higher than that of other immune genes (TLR-3, IL-1β, Type I IFN, Type II IFN and Mx gene) at 12dph, 18dph (Fig. 7A) and 50dph (Fig. 7B). These results indicate the fish were cultured in a healthy environment and did not contract infections.

4. Discussion

Assessment of the intestinal bacterial composition of healthy *E. coioides* can help to establish intestinal microbiota database and to identify potential gut probiotics. However, no such information is currently available. Here, we have performed assays on the intestinal microbiota and immune system associated with *E. coioides* at the pre-, mid-, and post-metamorphosis stages.

When the early development stage of grouper, the adaptive immunity is still not fully established and functioning; therefore the innate immunity has a crucial role in protect or fights to get rid of the pathogens, such as viruses, bacteria, and parasites [4,26,27]. The key cells of the innate immune system addressed here are NF-κB, TLR-3, IL-1β, Type I IFN, Type II IFN and Mx gene. NF-κB is an important

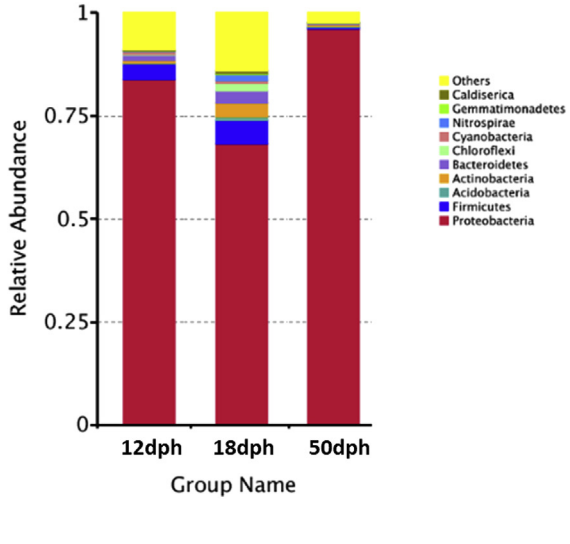

A

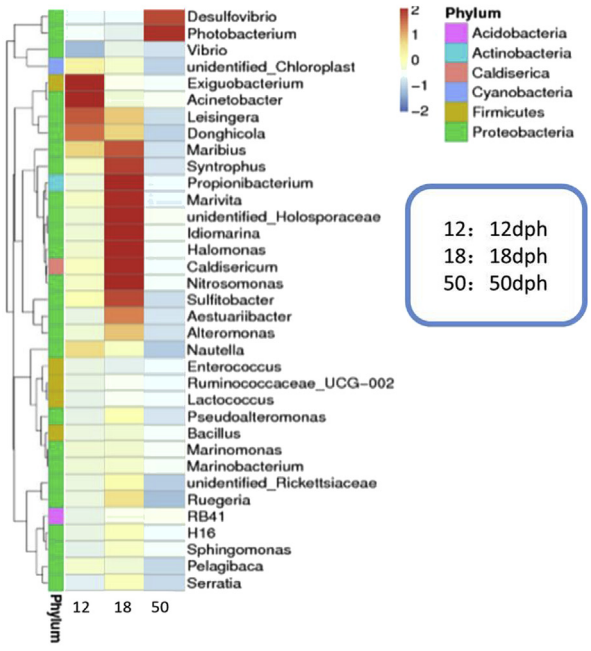

B

Fig. 4. The species and genera level of intestinal microbiomes in different metamorphosis stages. (A) The top 10 species in the different taxonomic ranks were selected to form the distribution histogram of relative abundance. Plotted by the "Relative Abundance" on the Y-axis and "Samples Name" on the X-axis. "Others" represents a total relative abundance of the rest phylum besides the top 10 phylum. (B) The abundance distribution of dominant 35 genera among all samples was displayed in the species abundance heatmap. Plotted by sample name on the X-axis and the Y-axis represents the genus. Red color represented most abundance and blue color represented less abundance. (For interpretation of the references to color in this figure legend, the reader is referred to the Web version of this article.)

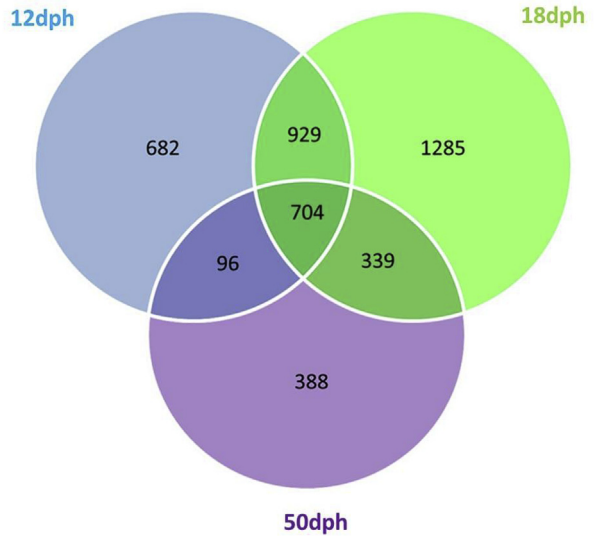

Fig. 5. Venn diagram: the OTUs in each metamorphosis stages (12dph, 18dph and 50sph) are 682, 1285 and 50dph, respectively. According to the analysis results of OTUs clustering, the common information of the grouper in three different development stages is 704 OTUs.

transcription factor that responds to various stimuli. NFκB is typically inactive and remains sequestered in the cytoplasm under nonstress-related conditions [28]. When NF-κB is activated, it will regulate the suppression of cellular apoptosis. On the other hands, toll-like receptors (TLRs) family are a key pathogen recognition receptors (PRRs), starting up the antivirus signaling pathway [29]. Virus-infected cell secretes interferon, which induce nearby uninfected cells to produce substances that inhibit viral reproduction and transported by the blood stream to alarm other cells in the body [30]. IFNs are a family of structurally related cytokines with a hallmark function of antiviral activity [31]. Interleukin-1β (IL-1β) is an endogenous pyrogen produced and released at the early stage response following infections, and subsequently considered as initiator of the pro-inflammatory response in macrophages, activator of lymphocytes and a synthesis promoter of other cytokines and prostaglandins [32,33].

In this study, the alpha diversity analysis indicates the intestinal microbiota communities in grouper larvae (12 and 18 dph) is richer than those in the juveniles (50dph). Similar result has been observed in *Arapaima gigas* and *Gadus morhuathat* [34,35]. Interestingly, the intestinal microbiota in blunt snout bream (*Megalobrama amblycephala*) is altered during feeding habit transition [36]. All together, these results show that the richness and diversity of intestinal bacterial communities are subjected to the influence of development, feeding habit, and environments. Importantly, we have found profound differences in the intestinal microbial compositions among the grouper at pre-, mid-, and post-metamorphosis stages. The observation raises an interesting question about the impact of the different microbial compositions on the fish going through this critical transformation stage.

In this study, we have shown significant variations in the abundance and diversity of intestinal microbiota in grouper at different developmental stages. The most prevalent phylum is the gram-negative *Proteobacteria*, which often are the most dominant phylum in the intestine of numerous marine fish, including *Plectropomus leopardus*, *Seriola lalandi Ctenopharyngodon idellus*, *Megalobrama amblycephala*, *Carassius auratus*, and *Hypophthalmichthys nobilis* [37–39]. In *Oncorhynchus mykiss*, *Proteobacteria* can make up over 70% of the total population [40,41]. Next to *Proteobacteria* was the phylum of *Firmicutes*, which took up 4% and 6% of the total population in the larvae at 12dph and 18dph, respectively. Similar observation has been reported previously in farm and aquarium rainbow trout. Both *Firmicutes* and *Proteobacteria* are proficient in fermentation of carbohydrates and proteins, and thus promote nutrients uptake by host from the diets [42].

A number of intestinal bacteria identified in the grouper guts may be worth further investigation for their beneficial effects on the fish. At genus level, *Exiguobacterium* was most abundant in the intestine at 12dph. Dominance of *Exiguobacterium* in fish at early life stage has also been reported in African turquoise killifish (6 weeks). *Exiguobacterium* has been reported to be anti-inflammatory mediator [43], and has been applied by the industry on bioremediation and degradation of toxic substances released into the environments [44]. Another dominant species, *Acinetobacter*, is known for therapeutic functions, including

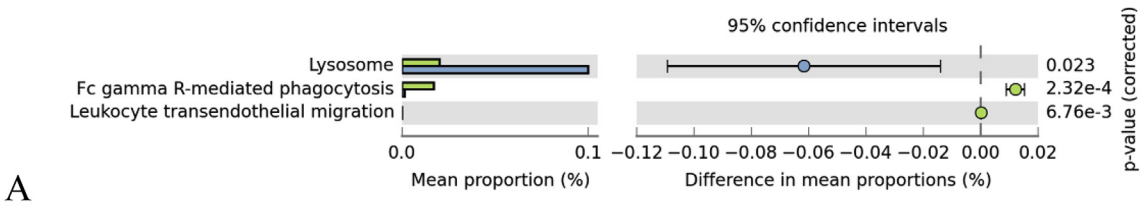

A

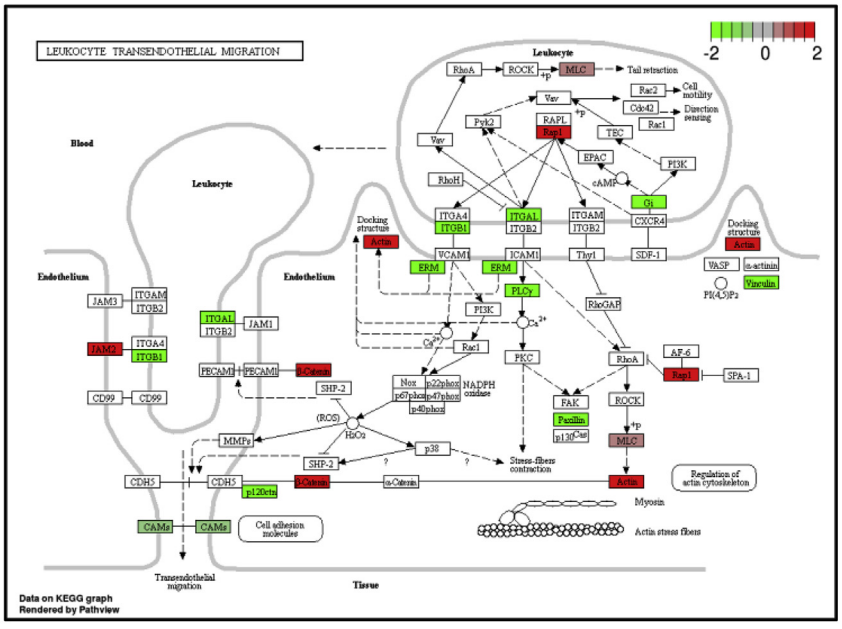

B

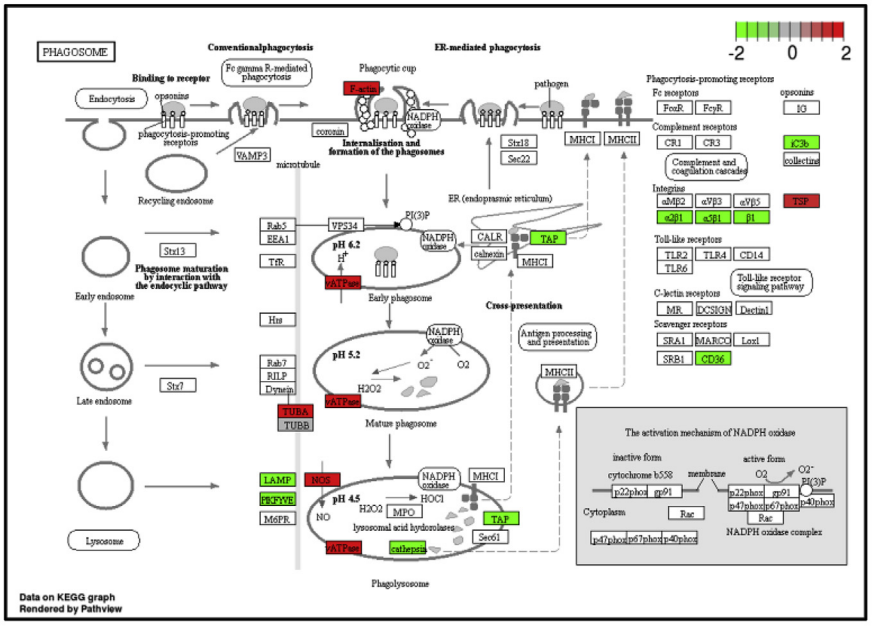

C

Fig. 6. The functional pathway observed by 16s rRNA gene sequencing and transcriptome analysis. (A) 16s rRNA gene sequencing: the functional changes in the microbiome of 12dph and 50dph. KEGG pathway (level 3) indicates statistically significant differences between the two data sets (p-value < 0.05). (B) The analysis of gene expression in leukocyte transendothelial migration pathway through KEGG. This pathway shows the migration of leukocyte from blood into tissue by going through the cell junction between endothelium cells. The up-regulated genes were labelled with red, while the down-regulated genes were labelled with green. (C) The analysis of gene expression in phagosome pathway through KEGG. The up-regulated genes were labelled with red, while the down-regulated genes were labelled with green. (For interpretation of the references to color in this figure legend, the reader is referred to the Web version of this article.)

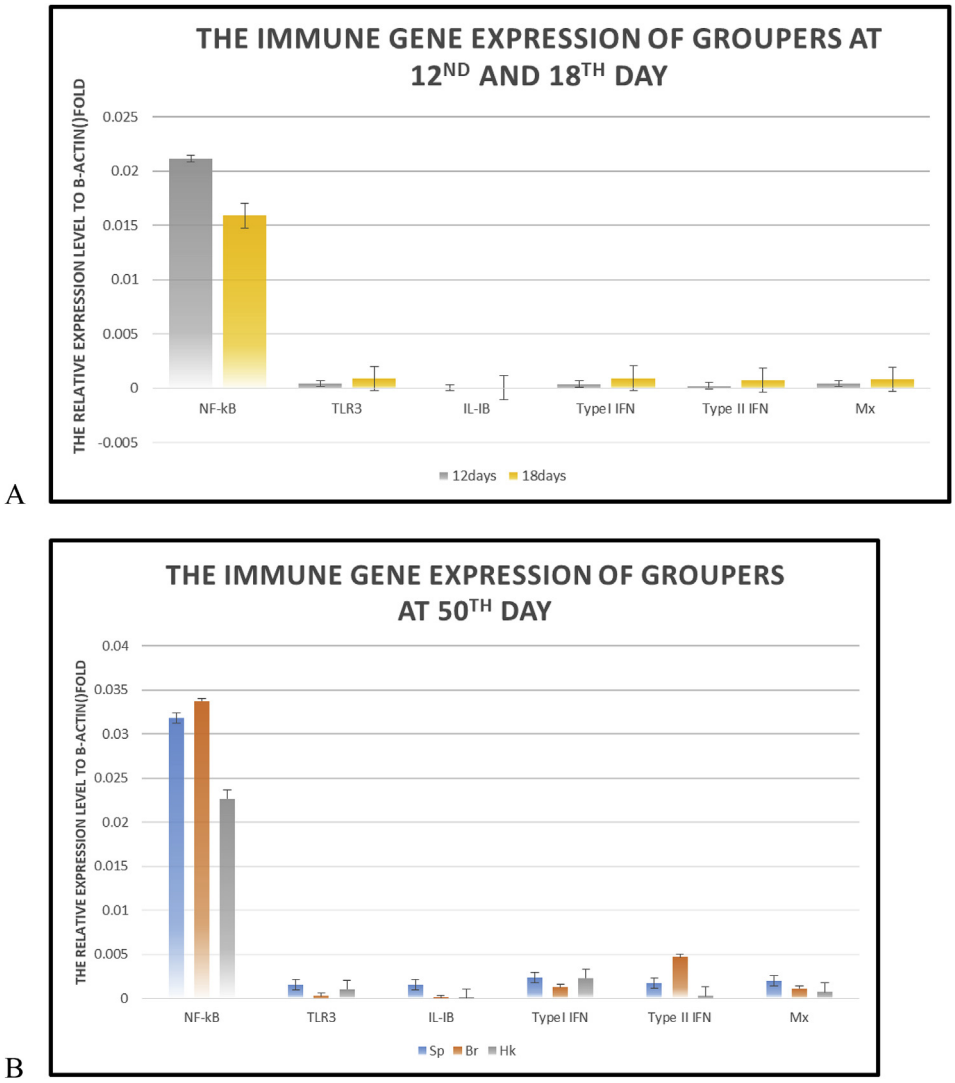

Fig. 7. The expression of immune genes (NF-κB, TLR-3, IL-1β, Type I IFN, Type II IFN and Mx gene) was determined by real-time PCR. NF-κB was slightly higher than the other immune genes (TLR-3, IL-1β, Type I IFN, Type II IFN and Mx gene) at 12dph, 18dph (A) and 50dph (B).

antibacterium, antivirus, anticancer, insecticide, and enzyme inhibition [45,46]. Hence, the intestinal *Acinetobacter* might play a major role in protecting hosts from microbial infection at their early life stage. The gut content of 18dph-grouper was dominated by seven major genera, that is, *Propionibacterium*, *Marivita, unidentified-Holosporacaea*, *Idiomarinas*, *Halomonas*, *Caldisericum* and *Nitrosomonas.* Among these species, *Caldisericum* is known to be important in the oxidation of reduced sulfur species because the growth of *Caldisericum* occurs with anaerobic respiration using sulfur compounds [47]. In aquaculture, *Nitrosomonas* is well-known as ammonia oxidizer that converts ammonia (NH_3) into nitrite (NO^{2-}), and can be applied to reduce the toxicity in water by turning NH_3 to NO^{2-} [48]. It will be interesting to further explore these bacteria mentioned above for potential applications on improvements on water quality or host health.

The KEGG pathway analysis has revealed several pathways and molecules that might play important roles in mediating immunity in grouper at pre-, mid-, and post-metamorphosis stage. In particular, the expression of several molecules in the leukocyte transendothelial migration pathway was significantly regulated in the grouper at different stages (Fig. 6B). CDH5 is a classical cadherin important to the formation of cell junctions [49]. Meanwhile, p120ctn, which was down-regulated, is a component in cadherin-catenin complex that helps to stabilize cadherin on cell membrane and regulates cytoskeletal re-organization leading to junction maturation [50,51]. p120ctn and CDH5 forms a complex which could affect the expression of β-catenin. In Fig. 6B, β-catenin was found to be upregulated and so was actin. β-catenin regulates cell growth and helps to form adherens junction, while actin builds up filament and cytoskeleton. β-catenin has been shown to affect actin through α-caterin, which binds directly to the actin filaments [52–54]. A small GTPase, Rap1, was also up-regulated. Rap1 can be activated by cytokines and neurotransmitters, and is involved in the regulation of cell-cell contact and the formation of adherens junctions especially in the contact between T cells and antigen-presenting cells (APC) [54–56]. JAM2, which was also up-regulated, is a vascular molecule in interendothelial junctional complexes and can also mediate cell-cell contact especially among immune cells [57,58]. In addition, JAM2 is involved in the process of lymphocyte homing to the secondary lymphoid organs and the regulation of transendothelial migration [58]. These data indicate that leukocyte transendothelial migration might be critical to the development of immune system in grouper going through the metamorphosis process. Further investigation will shed light on our understanding of the role of leukocyte transendothelial migration in the development of immune system in grouper.

Several genes in the phagosome pathway were also evidently regulated (Fig. 6C). F-actin, which was up-regulated, forms actin filaments to build cytoskeleton that helps in maintaining cell junction and

cell shape by remodeling cell cytoskeletal structures to form phagocytic cup [59]. TUBA, which was also upregulated, binds microtubules and builds cytoskeletal to provide structural support for cell during the remodeling of cell cytoskeletal. TUBA was found to be linked to actin through specific independent mechanism and may regulate actin in endocytosis [60]. The upregulation of vATPase on phagosome membrane might induce hydrogen ion to flow into the endosome, leading to acidosis in phagosome, a condition allowing lysosome to decompose. This result was similar to that of 16s rRNA metagenomic analysis (Fig. 6A). Future study is required to further illustrate the importance of phagosome pathway to the immunity in grouper throughout the metamorphosis process.

In summary, we have performed metagenomic and transcriptomic analyses to investigate the microbiota and immune system development in the intestines of grouper at three developmental stages: pre, mid-, and post-metamorphosis. The obtained information will not only increase our knowledge of the development of grouper, but also assist in developing strategy to enhance health in fish going through the critical metamorphosis stage. For example, manipulating the gut microbiomes to resemble a community found in the healthy grouper might enhance the immunity against infections.

Acknowledgements

This study was financially supported by Ministry of Science and Technology (grant number:MOST-107-2321-B-019-002). We would like to acknowledge Biotools, Co., Ltd for assistance with analyzing the 16s rRNA metagenomics.

References

[1] L.-S. Lim, Y. Mukai, Morphogenesis of sense organs and behavioural changes in larvae of the brown-marbled grouper Epinephelus fuscoguttatus(Forsskål), Mar. Freshw. Behav. Physiol. 47 (5) (2014) 313–327.
[2] Y.Y. Chen, A.C. Cheng, S.A. Cheng, J.C. Chen, Orange-spotted grouper Epinephelus coioides that have encountered low salinity stress have decreased cellular and humoral immune reactions and increased susceptibility to Vibrio alginolyticus, Fish Shellfish Immunol. 80 (2018) 392–396.
[3] A.T. Gonçalves, C. Gallardo-Escárate, Microbiome dynamic modulation through functional diets based on pre- and probiotics (mannan-oligosaccharides andSaccharomyces cerevisiae) in juvenile rainbow trout (Oncorhynchus mykiss), J. Appl. Microbiol. (2017) 1333–1347.
[4] A.E. Ellis, Innate host defense mechanisms of fish against viruses and bacteria, Dev. Comp. Immunol. 25 (8–9) (2001) 827–839.
[5] E. Thursby, N. Juge, Introduction to the human gut microbiota, Biochem. J. 474 (11) (2017) 1823–1836.
[6] M. Rosenthal, D. Goldberg, A. Aiello, E. Larson, B. Foxman, Skin Microbiota: Microbial Community Structure and its Potential Association with Health and Disease, Infection, Genetics and Evolution : Journal of Molecular Epidemiology and Evolutionary Genetics in Infectious Diseases, (2011), pp. 839–848.
[7] S. Virtanen, I. Kalliala, P. Nieminen, A. Salonen, Comparative analysis of vaginal microbiota sampling using 16S rRNA gene analysis, PLoS One (2017) e0181477.
[8] A.M. O'Hara, F. Shanahan, The gut flora as a forgotten organ, EMBO Rep. 7 (7) (2006) 688–693.
[9] I. Sekirov, S.L. Russell, L.C. Antunes, B.B. Finlay, Gut microbiota in health and disease, Physiol. Rev. 90 (3) (2010) 859–904.
[10] J.M. Wong, R. de Souza, C.W. Kendall, A. Emam, D.J. Jenkins, Colonic health: fermentation and short chain fatty acids, J. Clin. Gastroenterol. 40 (3) (2006) 235–243.
[11] F. De Vadder, P. Kovatcheva-Datchary, D. Goncalves, J. Vinera, C. Zitoun, A. Duchampt, F. Backhed, G. Mithieux, Microbiota-generated metabolites promote metabolic benefits via gut-brain neural circuits, Cell 156 (1–2) (2014) 84–96.
[12] M. Carabotti, A. Scirocco, M.A. Maselli, C. Severi, The gut-brain axis: interactions between enteric microbiota, central and enteric nervous systems, Ann. Gastroenterol.: Quart. Publ. Hellenic Soc. Gastroenterol. 28 (2) (2015) 203–209.
[13] J.A. Foster, K.A. McVey Neufeld, Gut-brain axis: how the microbiome influences anxiety and depression, Trends Neurosci. 36 (5) (2013) 305–312.
[14] A.K. Fleck, D. Schuppan, H. Wiendl, L. Klotz, Gut-CNS-Axis as possibility to modulate inflammatory disease activity-implications for multiple sclerosis, Int. J. Mol. Sci. 18 (7) (2017).
[15] R. Cianci, D. Pagliari, C.A. Piccirillo, J.H. Fritz, G. Gambassi, The microbiota and immune system crosstalk in health and disease, Mediat. Inflamm. 2018 (2018) 1–3.
[16] S. Rautava, R. Luoto, S. Salminen, E. Isolauri, Microbial contact during pregnancy, intestinal colonization and human disease, Nat. Rev. Gastroenterol. Hepatol. 9 (10) (2012) 565–576.
[17] S. Mazumdar-Leighton, V.K. Choudhary, Metagenomics at grass roots, Resonance 22 (3) (2017) 291–301.
[18] N. Youssef, C.S. Sheik, L.R. Krumholz, F.Z. Najar, B.A. Roe, M.S. Elshahed, Comparison of species richness estimates obtained using nearly complete fragments and simulated pyrosequencing-generated fragments in 16S rRNA gene-based environmental surveys, Appl. Environ. Microbiol. 75 (16) (2009) 5227–5236.
[19] M. Hess, A. Sczyrba, R. Egan, T.W. Kim, H. Chokhawala, G. Schroth, S. Luo, D.S. Clark, F. Chen, T. Zhang, R.I. Mackie, L.A. Pennacchio, S.G. Tringe, A. Visel, T. Woyke, Z. Wang, E.M. Rubin, Metagenomic discovery of biomass-degrading genes and genomes from cow rumen, Science 331 (6016) (2011) 463–467.
[20] F. Asnicar, G. Weingart, T.L. Tickle, C. Huttenhower, N. Segata, Compact graphical representation of phylogenetic data and metadata with GraPhlAn, PeerJ 3 (2015).
[21] T.Z. DeSantis, P. Hugenholtz, K. Keller, E.L. Brodie, N. Larsen, Y.M. Piceno, R. Phan, G.L. Andersen, NAST: a multiple sequence alignment server for comparative analysis of 16S rRNA genes, Nucleic Acids Res. 34 (Web Server) (2006) W394–W399.
[22] B.D. Ondov, N.H. Bergman, A.M. Phillippy, Interactive metagenomic visualization in a Web browser, BMC Bioinf. 12 (1) (2011).
[23] D. Bulgarelli, R. Garrido-Oter, Philipp C. Münch, A. Weiman, J. Dröge, Y. Pan, Alice C. McHardy, P. Schulze-Lefert, Structure and function of the bacterial root microbiota in wild and domesticated barley, Cell Host Microbe 17 (3) (2015) 392–403.
[24] B. Li, X. Zhang, F. Guo, W. Wu, T. Zhang, Characterization of tetracycline resistant bacterial community in saline activated sludge using batch stress incubation with high-throughput sequencing analysis, Water Res. 47 (13) (2013) 4207–4216.
[25] E. Avershina, T. Frisli, K. Rudi, De novo semi-alignment of 16S rRNA gene sequences for deep phylogenetic characterization of next generation sequencing data, Microb. Environ. 28 (2) (2013) 211–216.
[26] P.K. Sahoo, P.K. Meher, K.D. Mahapatra, J.N. Saha, R.K. Jana, P.V.G.K. Reddy, Immune responses in different fullsib families of Indian major carp, Labeo rohita, exhibiting differential resistance to Aeromonas hydrophila infection, Aquaculture 238 (1–4) (2004) 115–125.
[27] Y.-C. Yeh, Y.-J. Hsu, Y.-M. Chen, H.-Y. Lin, H.-L. Yang, T.-Y. Chen, H.-C. Wang, EcVig, a novel grouper immune-gene associated with antiviral activity against NNV infection, Dev. Comp. Immunol. 43 (1) (2014) 68–75.
[28] K.-M. Debatin, Apoptosis pathways in cancer and cancer therapy, Cancer Immunol. Immunother. 53 (3) (2004) 153–159.
[29] R. Huo, X. Zhao, J. Han, T. Xu, Genomic organization, evolution and functional characterization of soluble toll-like receptor 5 (TLR5S) in miiuy croaker (Miichthys miiuy), Fish Shellfish Immunol. 80 (2018) 109–114.
[30] R.E. Randall, S. Goodbourn, Interferons and viruses: an interplay between induction, signalling, antiviral responses and virus countermeasures, J. Gen. Virol. 89 (1) (2008) 1–47.
[31] M.-W.W. Lu, Jen-Leih, Innate immune response of NNV infection in fish and its disease prevention, J. Mar. Biosci. Biotechnol. 2 (Issue 3) (2007) 127–132.
[32] P. Alvarez-Pellitero, Fish immunity and parasite infections: from innate immunity to immunoprophylactic prospects, Vet. Immunol. Immunopathol. 126 (3–4) (2008) 171–198.
[33] C.A. Dinarello, Immunological and inflammatory functions of the interleukin-1 family, Annu. Rev. Immunol. 27 (1) (2009) 519–550.
[34] G. do Vale Pereira, D.G. da Cunha, J.L. Pedreira Mourino, A. Rodiles, A. Jaramillo-Torres, D.L. Merrifield, Characterization of microbiota in Arapaima gigas intestine and isolation of potential probiotic bacteria, J. Appl. Microbiol. 123 (5) (2017) 1298–1311.
[35] T. Forberg, E.B. Sjulstad, I. Bakke, Y. Olsen, A. Hagiwara, Y. Sakakura, O. Vadstein, Correlation between microbiota and growth in mangrove killifish (Kryptolebias marmoratus) and Atlantic cod (Gadus morhua), Sci. Rep. 6 (1) (2016).
[36] J. Wei, X. Guo, H. Liu, Y. Chen, W. Wang, The variation profile of intestinal microbiota in blunt snout bream (Megalobrama amblycephala) during feeding habit transition, BMC Microbiol. 18 (1) (2018) 99.
[37] G.D. Alpini, M. Mekuchi, T. Asakura, K. Sakata, T. Yamaguchi, K. Teruya, J. Kikuchi, Intestinal microbiota composition is altered according to nutritional biorhythms in the leopard coral grouper (Plectropomus leopardus), PLoS One 13 (6) (2018).
[38] T.P.R.A. Legrand, S.R. Catalano, M.L. Wos-Oxley, F. Stephens, M. Landos, M.S. Bansemer, D.A.J. Stone, J.G. Qin, A.P.A. Oxley, The inner workings of the outer surface: skin and gill microbiota as indicators of changing gut health in Yellowtail Kingfish, Front. Microbiol. 8 (2018).
[39] I. Ortega Blázquez, M.J. Grande Burgos, R. Pérez-Pulido, A. Gálvez, R. Lucas, Treatment with high-hydrostatic pressure, activated film packaging with Thymol plus Enterocin AS-48, and its combination modify the bacterial communities of refrigerated sea bream (sparus aurata) fillets, Front. Microbiol. 9 (2018).
[40] C.J. Krediet, K.B. Ritchie, A. Alagely, M. Teplitski, Members of native coral microbiota inhibit glycosidases and thwart colonization of coral mucus by an opportunistic pathogen, ISME J. 7 (5) (2012) 980–990.
[41] O. Schildgen, Y. Zuo, W. Xie, Y. Pang, T. Li, Q. Li, Y. Li, Bacterial community composition in the gut content of Lampetra japonica revealed by 16S rRNA gene pyrosequencing, PLoS One 12 (12) (2017).
[42] P. Fan, P. Liu, P. Song, X. Chen, X. Ma, Moderate dietary protein restriction alters the composition of gut microbiota and improves ileal barrier function in adult pig model, Sci. Rep. 7 (2017) 43412.
[43] P. Smith, D. Willemsen, M. Popkes, F. Metge, E. Gandiwa, M. Reichard, D.R. Valenzano, Regulation of life span by the gut microbiota in the short-lived African turquoise killifish, eLife 6 (2017).
[44] R.C. Kasana, C.B. Pandey, Exiguobacterium: an overview of a versatile genus with potential in industry and agriculture, Crit. Rev. Biotechnol. 38 (1) (2018) 141–156.
[45] J.-S. Lee, Acinetobacter antiviralis sp. nov., from Tobacco plant roots, J. Microbiol. Biotechnol. 19 (3) (2009).
[46] S.A. Wadhwani, M. Gorain, P. Banerjee, U.U. Shedbalkar, R. Singh, G.C. Kundu,

B.A. Chopade, Green synthesis of selenium nanoparticles using Acinetobacter sp. SW30: optimization, characterization and its anticancer activity in breast cancer cells, Int. J. Nanomed. 12 (2017) 6841–6855.
[47] K. Mori, K. Yamaguchi, Y. Sakiyama, T. Urabe, K. Suzuki, Caldisericum exile gen. nov., sp. nov., an anaerobic, thermophilic, filamentous bacterium of a novel bacterial phylum, Caldiserica phyl. nov., originally called the candidate phylum OP5, and description of Caldisericaceae fam. nov., Caldisericales ord. nov. and Caldisericia classis nov, Int. J. Syst. Evol. Microbiol. 59 (Pt 11) (2009) 2894–2898.
[48] M.A. van Kessel, R.J. Mesman, A. Arshad, J.R. Metz, F.A. Tom Spanings, S.C. van Dalen, L. van Niftrik, G. Flik, S.E. Wendelaar Bonga, M.S. Jetten, P.H. Klaren, H.J. Op den Camp, Branchial Nitrogen Cycle Symbionts Can Remove Ammonia in Fish Gills, Environmental Microbiology Reports, (2016).
[49] S. Alimperti, S.T. Andreadis, CDH2 and CDH11 act as regulators of stem cell fate decisions, Stem Cell Res. 14 (3) (2015) 270–282.
[50] A. Kourtidis, S.P. Ngok, P.Z. Anastasiadis, p120 catenin: an essential regulator of cadherin stability, adhesion-induced signaling, and cancer progression, Progress Mole. biol. Transl. Sci. 116 (2013) 409–432.
[51] T. Pieters, F. van Roy, J. van Hengel, Functions of p120ctn isoforms in cell-cell adhesion and intracellular signaling, Front. Biosci. (Landmark edition) 17 (2012) 1669–1694.
[52] F. Drees, S. Pokutta, S. Yamada, W.J. Nelson, W.I. Weis, Alpha-catenin is a molecular switch that binds E-cadherin-beta-catenin and regulates actin-filament assembly, Cell 123 (5) (2005) 903–915.
[53] L.P. Elia, M. Yamamoto, K. Zang, L.F. Reichardt, p120 catenin regulates dendritic spine and synapse development through Rho-family GTPases and cadherins, Neuron 51 (1) (2006) 43–56.
[54] W.J. Nelson, Regulation of cell-cell adhesion by the cadherin-catenin complex, Biochem. Soc. Trans. 36 (Pt 2) (2008) 149–155.
[55] K. Katagiri, M. Hattori, N. Minato, T. Kinashi, Rap1 functions as a key regulator of T-cell and antigen-presenting cell interactions and modulates T-cell responses, Mol. Cell Biol. 22 (4) (2002) 1001–1015.
[56] A.L. Knox, N.H. Brown, Rap1 GTPase regulation of adherens junction positioning and cell adhesion, Science 295 (5558) (2002) 1285–1288.
[57] M. Aurrand-Lions, L. Duncan, C. Ballestrem, B.A. Imhof, JAM-2, a novel immunoglobulin superfamily molecule, expressed by endothelial and lymphatic cells, J. Biol. Chem. 276 (4) (2001) 2733–2741.
[58] C.A. Johnson-Leger, M. Aurrand-Lions, N. Beltraminelli, N. Fasel, B.A. Imhof, Junctional adhesion molecule-2 (JAM-2) promotes lymphocyte transendothelial migration, Blood 100 (7) (2002) 2479–2486.
[59] P. Rougerie, V. Miskolci, D. Cox, Generation of membrane structures during phagocytosis and chemotaxis of macrophages: role and regulation of the actin cytoskeleton, Immunol. Rev. 256 (1) (2013) 222–239.
[60] M.A. Salazar, A.V. Kwiatkowski, L. Pellegrini, G. Cestra, M.H. Butler, K.L. Rossman, D.M. Serna, J. Sondek, F.B. Gertler, P. De Camilli, Tuba, a novel protein containing bin/amphiphysin/Rvs and Dbl homology domains, links dynamin to regulation of the actin cytoskeleton, J. Biol. Chem. 278 (49) (2003) 49031–49043.